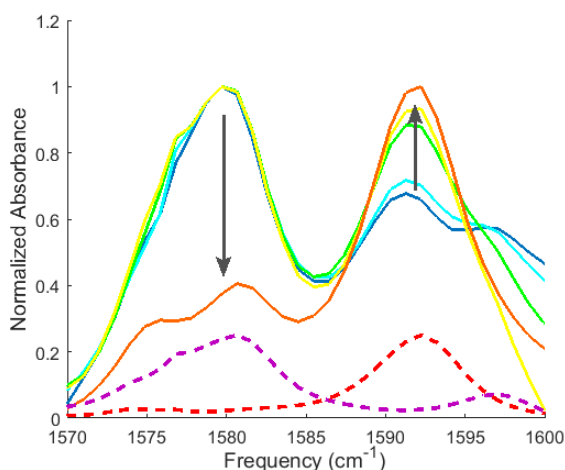


## Research Progress

Asphaltenes, represent the most polar and aromatic components of petroleum and are specifically defined by their solubility in benzene and toluene and insolubility in n-heptane and n-pentane. The presence of asphaltenes in petroleum can substantially reduce oil performance and refining yields due to their high viscosities and propensity to aggregate and phase separate. Typically, asphaltene inhibitors are employed during the extraction process in order to disrupt aggregation and prevent flocculation. While a variety of inhibitor designs exist, the basic structure can be divided into a polar head group to specifically target the asphaltenes and a nonpolar tail group to stabilize the complexed asphaltene-inhibitor structure in the surrounding nonpolar oil medium. Thus, inhibitor performance is critically linked to the affinity of asphaltenes towards the inhibitor head group. However, the complex and wide variety of asphaltene structures (island and archipelago) and heteroatoms (N, S, O) presents a substantial challenge to developing a comprehensive assessment of inhibitor performance. This research investigates the chemistry of asphaltene-inhibitor interactions through the use self-assembled nonaqueous reverse micelle (RM) structures. Specifically, we aim to: 1) determine inhibitor affinities and binding mechanisms using heteroatom proxies of asphaltene molecules, 2) investigate the influence of asphaltene architecture on inhibitor affinity, 3) and quantify the impact of resin fractions on asphaltene stabilization.



**Figure 2.** Infrared absorption spectra of pyridine in AOT RMs containing EG cores. Pyridine spectra in various RM size and core and surrounding solvents are denoted as follows:  $w_s = 0.5$  (blue),  $w_s = 1.0$  (teal),  $w_s = 2.0$  (green),  $w_s = 3.0$  (yellow),  $w_s = 4.0$  (orange), heptane (dashed purple), and EG (dashed red).

pyridine-doped EG/AOT RMs prepared at various sizes based on the  $w_s = [EG]/[AOT]$  ratio are displayed in Figure 2. For  $w_s = 0.5$  the IR spectrum shows a peak in the  $1592\text{ cm}^{-1}$  region suggesting that some of the pyridine is located within the RMs. However, this peak is overshadowed by a larger peak located at  $1580\text{ cm}^{-1}$ , indicative of unbound pyridine localized in the nonpolar heptane. As RM size increases the spectral contribution from the hydrogen-bound

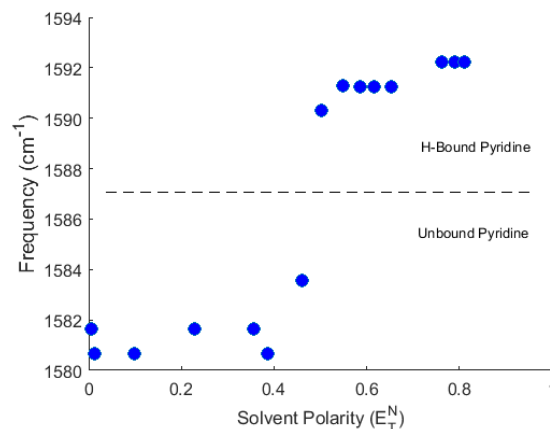


**Figure 1.** Infrared absorption transition frequencies of pyridine as a function of normalized solvent polarity ( $E_T^N$ ).

To address these challenges, we have directed our early studies to properties of pyridine. Pyridine possesses a conjugated, cyclic structure along with a nitrogen heteroatom, making it an ideal proxy of a heteroatom site within a larger asphaltene structure. Figure 1 displays the IR absorption transition frequencies of pyridine in various organic solvents as a function of the normalized solvent polarity parameter ( $E_T^N$ ). In aprotic solvents transition frequencies range from  $1581\text{--}1584\text{ cm}^{-1}$ , while in protic solvents the transition shifts dramatically up to  $1590\text{--}1593\text{ cm}^{-1}$ . Based on these observations we have assigned the spectral region of  $1590\text{--}1593\text{ cm}^{-1}$  as pyridine hydrogen-bound to the surrounding solvent. Similarly, the  $1581\text{--}1584\text{ cm}^{-1}$  region corresponds to “free” or unbound pyridine.

The ability distinguish between hydrogen-bound and unbound version of pyridine has been critical tool for examining pyridine doped within RMs. We have specifically focused on RMs with ethylene glycol (EG) as our polar organic solvent, sodium bis(2-ethylhexyl) sulfosuccinate (AOT) as the surfactant, and heptane as the nonpolar phase. The IR spectra of

pyridine also increases, suggesting that a larger fraction of the available pyridine localized within the RM. At  $w_s = 4.0$  the spectral signature for unbound pyridine sharply decreases and the hydrogen-bound signature becomes the dominant spectral feature. Based on these observations it appears that there is critical RM at which pyridine is more readily incorporated into the RM interior. We are currently working towards quantifying the ratios of bound and unbound pyridine in order to better understand the operative factors directing pyridine incorporation. We have also been pursuing studies of pyridine doped RMs using NMR in order to quantify the pyridine to AOT distance.

Our studies have also allowed us to explore the properties of nonaqueous RMs. Numerous studies of aqueous RMs have used a core-shell or core-interfacial model to partition the aqueous interior. The interfacial region is distinguished as having a unique infrared absorption spectrum, a longer vibrational lifetime, slower orientation dynamics, and a more rigid hydrogen-bonding network compared to the bulk-like core  $H_2O$ . In contrast, nonaqueous RMs are thought to possess a continuous polar interior phase, without any core-interfacial distinctions. Figure 3 presents the IR absorption spectra of EG within AOT RMs in the O-H stretch region. The O-H stretch of EG in a  $w_s = 0.5$  RM is blue shifted and narrow relative to neat EG. As the  $w_s$  ratio increases the IR spectra gradually red shift and broaden, converging toward neat EG. However, the spectra never fully converge, suggesting that a distinct interfacial species of EG may be present with AOT RMs and that a core-interfacial model may indeed be appropriate for describing the polar interior. Current work is underway to quantify the partitioning between interfacial and core EG species. These studies will continue to inform our studies of heteroatom-doped nonaqueous RMs.

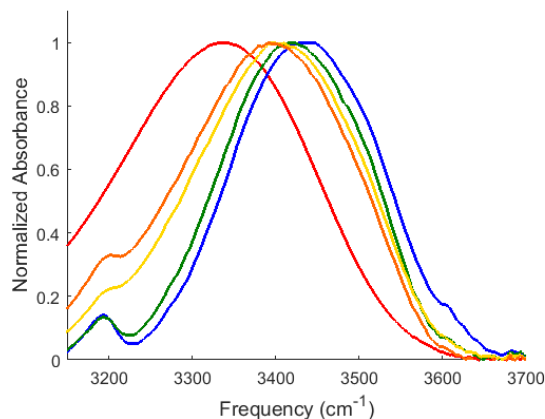


**Figure 3.** Normalized infrared absorption spectra of EG within AOT RMs. Spectra are denoted as follows:  $w_s = 0.5$  (blue),  $w_s = 1.0$  (green),  $w_s = 2.0$  (yellow),  $w_s = 3.0$  (orange), and EG (red).

### Career Development

Financial support from ACS PRF has been used to provide research opportunities for 3 undergraduate students at CNU and 1 local high school student. Beyond supporting research through the purchase of materials, this grant also provided 3 paid summer research opportunities. All 3 students (Fadah, Lindholm, and Tucker) are returning students and plan to continue their research throughout the 2018-2019 academic year.

One of the most rewarding aspects of this grant has been the ability to provide a summer research experience to a local high school student (Zaaheem McCall, Warwick High School), through the ACS Project SEED. Project SEED connects economically disadvantaged students with impactful research opportunities. While Project SEED provided financial support for Zaaheem, I would not have been able to provide the material support for Zaaheem's summer research project without the funds provided by ACS PRF. Zaaheem will be applying to colleges this Fall with hopes of pursuing a career in civil engineering.

Receiving the ACS PRF grant has had a profound impact on my career. During the 2017-2018 academic year I was awarded promotion to association professor with tenure. ACS PRF has played a critical role in demonstrating my own research potential and scholarship. This Fall my students and I will present our research at the Southeastern Regional Meeting of the ACS (SERMACS).